

# Dynamic Wetting Failure in Shear-Thinning and Shear-Thickening Liquids

Vasileios Charitatos,<sup>1</sup> Wieslaw J. Suszynski,<sup>1</sup> Marcio S. Carvalho,<sup>2</sup> and Satish Kumar<sup>1,\*</sup>

<sup>1</sup>Department of Chemical Engineering and Materials Science, University of Minnesota, Minneapolis, MN 55455, USA

<sup>2</sup>Department of Mechanical Engineering, Pontificia Universidade Católica do Rio de Janeiro, Rio de Janeiro, RJ 22451-900, Brazil

This document provides supplementary material on the rescaling of the data shown in figure 8, figure 12, figure 13, and figure 15 of the primary article “Dynamic Wetting Failure in Shear-Thinning and Shear-Thickening Liquids”.

## 1 Steady-state solution families

In figure 1a, the solution families of figure 8a of the primary article are replotted using  $Ca/Ca^{crit}$ . The families collapse onto a single curve, suggesting that the mechanism for dynamic wetting failure is similar in Newtonian and shear-thinning liquids. In figure 1b, the solution families of figure 8b of the primary article are replotted using  $Ca/Ca^{crit}$ . The families collapse onto a single curve, suggesting that the mechanism for dynamic wetting failure is similar in Newtonian and shear-thickening liquids.

## 2 Stress-gradient magnitude

The magnitudes of the stress gradients shown in figures 12a and 12b of the primary article are rescaled with their respective critical values and replotted using  $Ca/Ca^{crit}$  in figures 2a and 2b, respectively. In figure 2a, the magnitudes of the capillary-stress gradients of the Newtonian and shear-thinning liquids collapse on a single curve and so do the magnitudes of the receding-phase pressure gradients. For the shear-thickening liquid, the magnitudes

---

\*Email address for correspondence: kumar030@umn.edu

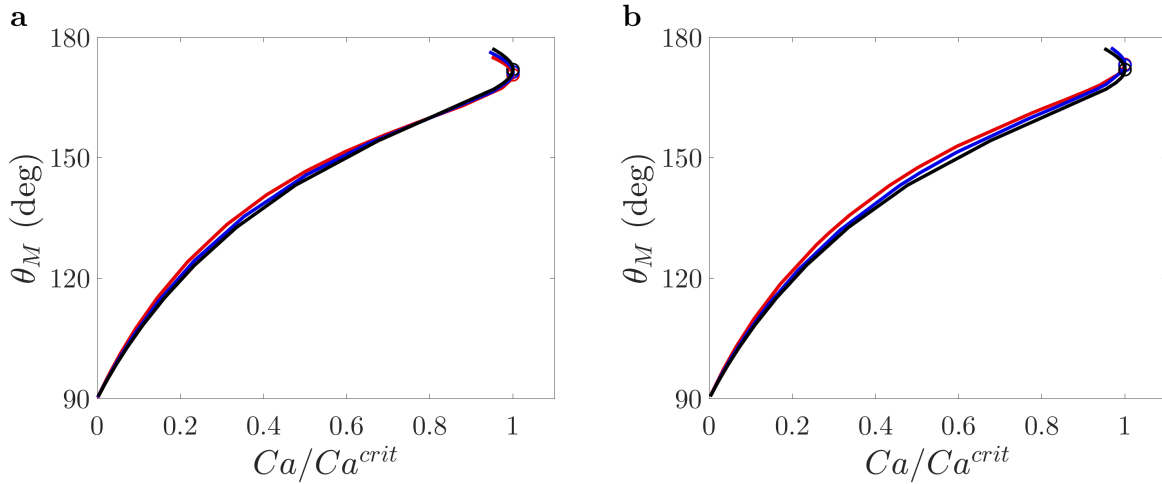


Figure 1: Solution families of (a) figure 8a and (b) figure 8b of the primary article replotted using  $Ca/Ca^{crit}$ .

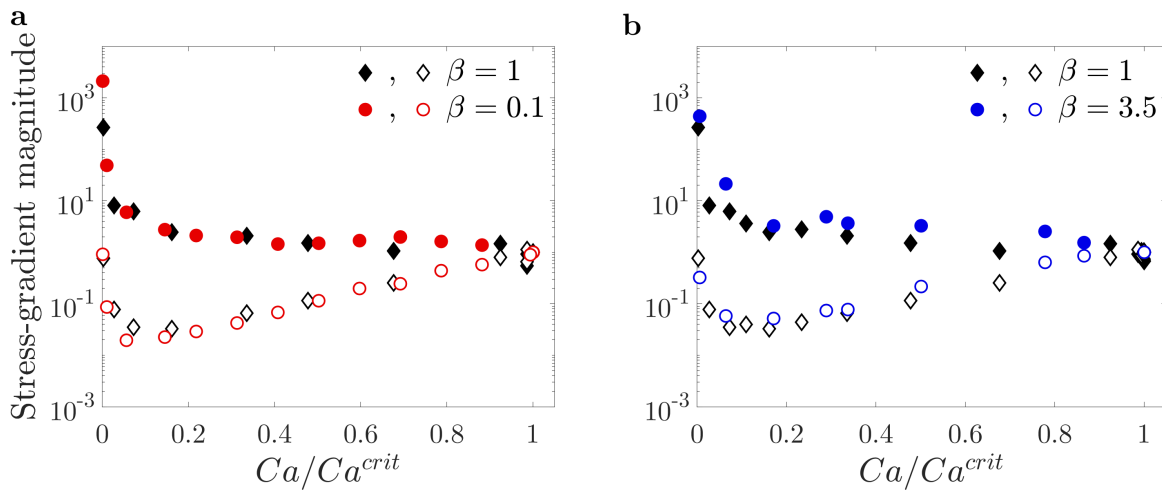


Figure 2: Stress-gradient magnitudes of (a) figure 12a and (b) figure 12b of the primary article rescaled with their respective critical values and replotted using  $Ca/Ca^{crit}$ . Filled symbols are the capillary-stress gradients, and open symbols are the receding-phase pressure gradients.

of the stress gradients behave similarly, as shown in 2b. This data collapse suggests that the underlying mechanism of dynamic wetting failure is similar for Newtonian, shear-thinning, and shear-thickening liquids. Note that in figures 2a and 2b, the dashed lines appearing in figures 12a and 12b of the primary article have been omitted for clarity.

### 3 Tangential stresses

In figure 3a, the tangential stresses for  $\beta = 0.1$  and  $\beta = 1$  shown in figure 13a of the primary article are rescaled by their respective critical values (values at  $Ca = Ca^{crit}$ ). The  $x$ -axis is also rescaled by  $Ca^{crit}$ . The data nearly collapse onto a single curve, suggesting that the mechanism of dynamic wetting failure is very similar for Newtonian and shear-thinning liquids.

The same analysis is conducted for the tangential stresses for  $\beta = 1$  and  $\beta = 3.5$  shown in figure 13b of the primary article. If the axes are rescaled as in figure 3a, the data nearly collapse onto a single curve as shown in figure 3b. This suggests that the mechanism of dynamic wetting failure is very similar for Newtonian and shear-thickening liquids. Note that in both figures 3a and 3b, the dashed lines shown in figures 13a and 13b of the primary article are omitted for clarity.

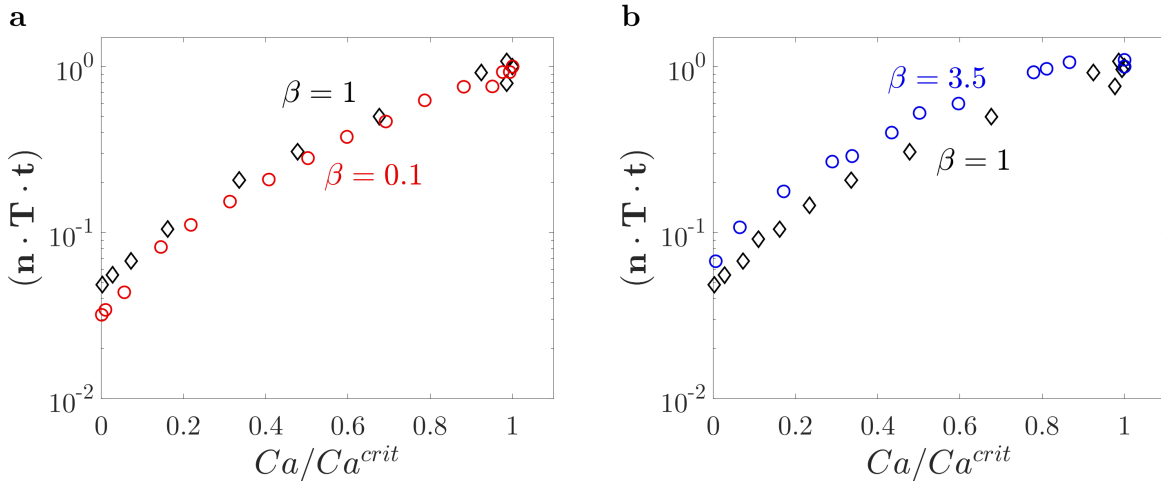


Figure 3: Magnitude of rescaled tangential stresses at the inflection point for (a) Newtonian liquid ( $\beta = 1$ , black diamonds), shear-thinning liquid ( $\beta = 0.1$ , red circles) and (b) Newtonian liquid ( $\beta = 1$ , black diamonds), shear-thickening liquid ( $\beta = 3.5$ , blue circles).

### 4 Characteristic length scales

The characteristic length scales  $h_f$  and  $r_f$  for  $\beta = 0.1$  and  $\beta = 1$  appearing in figure 15a of the primary article are rescaled with their respective critical values and replotted as a

function of  $Ca/Ca^{crit}$  in figure 4a. The  $r_f$  curves for the two liquids have a similar shape, and the same is true for the  $h_f$  curves.

In figure 4b, the characteristic length scales  $h_f$  and  $r_f$  for  $\beta = 1$  and  $\beta = 3.5$  appearing in figure 15b of the primary article are rescaled with their respective critical values and replotted as a function of  $Ca/Ca^{crit}$ . As in figure 4a, the  $r_f$  curves for both liquids have a similar shape, as do the  $h_f$  curves.

In figure 4c, the interface lengths  $L$  shown in figure 15c of the primary article for the three liquids are rescaled with their respective critical values and replotted as a function of  $Ca/Ca^{crit}$ . The data for all three liquids nearly collapse onto a single curve.

In figure 4d, the heights of the inflection point  $h_f$  shown in figure 15d of the primary article for the three liquids, are rescaled with their respective critical values and replotted with the interface lengths  $L$  rescaled with their respective critical values. The curves all have a similar shape. The rescalings shown in figure 4 support the idea that the mechanism for dynamic wetting failure in shear-thinning and shear-thickening liquids is similar to that in Newtonian liquids.

The characteristic length scales  $h_f$  and  $r_f$  for  $\beta = 0.1$  and  $\beta = 1$  appearing in figure 15a of the primary article are also rescaled with their respective maximum values and replotted as a function of  $Ca_{eff}$  in figure 5a. The  $r_f$  curves for the two liquids have a similar shape, and the same is true for the  $h_f$  curves.

In figure 5b, the characteristic length scales  $h_f$  and  $r_f$  for  $\beta = 1$  and  $\beta = 3.5$  appearing in figure 15b of the primary article are rescaled with their respective maximum values and replotted as a function of  $Ca_{eff}$ . Both the  $r_f$  and  $h_f$  data for the two liquids collapse onto two curves, respectively.

The interface lengths  $L$  shown in figure 15c of the primary article for the three liquids are rescaled with their respective maximum values and replotted as a function of  $Ca_{eff}$  in figure 5c. The data nearly collapse onto a single curve. However, the collapse is not as good as in figure 4c.

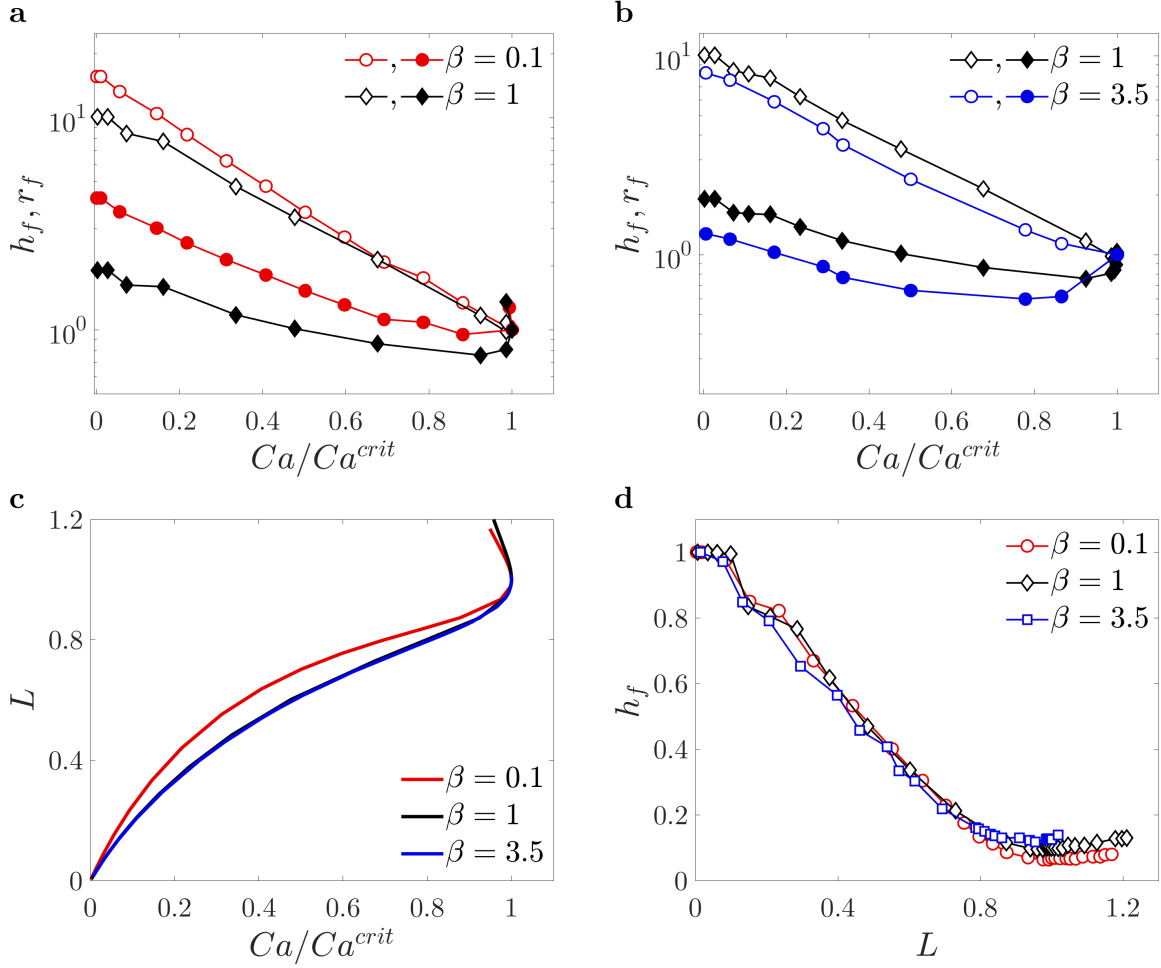


Figure 4: Black symbols are used for the Newtonian ( $\beta = 1$ ), red for shear-thinning ( $\beta = 0.1$ ), and blue for shear-thickening ( $\beta = 3.5$ ) liquids. (a)-(b) Rescaled interfacial length scales  $h_f$  (open symbols) and  $r_f$  (closed symbols) as a function of  $Ca/Ca^{crit}$ . (c) Rescaled interface length  $L$  as a function of  $Ca/Ca^{crit}$ . (d) Rescaled height of inflection point  $h_f$  as a function of rescaled interface length  $L$ .

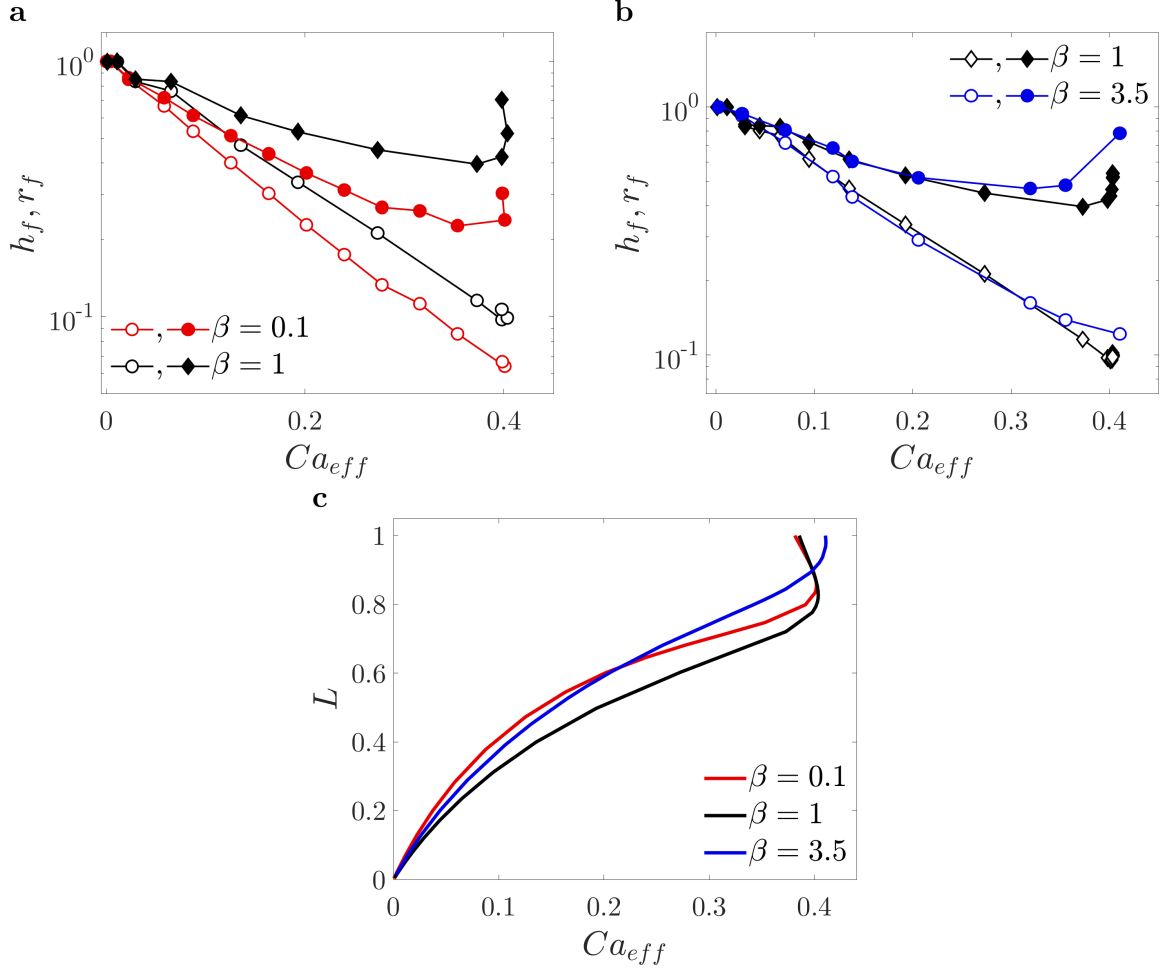


Figure 5: Black symbols are used for the Newtonian ( $\beta = 1$ ), red for shear-thinning ( $\beta = 0.1$ ), and blue for shear-thickening ( $\beta = 3.5$ ) liquids. (a)-(b) Rescaled interfacial length scales  $h_f$  (open symbols) and  $r_f$  (closed symbols) as a function of  $Ca_{eff}$ . (c) Rescaled interface length  $L$  as a function of  $Ca_{eff}$ .